ORIGINAL ARTICLE



New insights into the binding of PF4 to long heparin oligosaccharides in ultralarge complexes using mass spectrometry

Deling Shi^{1,2} | Huimin Zhao¹ | Changkai Bu¹ | Keith Fraser^{2,3} | Haoran Wang¹ | Jonathan S. Dordick^{2,3,4,5} | Robert J. Linhardt^{2,3,4,6} | Fuming Zhang^{2,4} | Feng Shi⁷ | Lianli Chi¹

¹National Glycoengineering Research Center, Shandong University, Qingdao, Shandong Province, China

²Center for Biotechnology and Interdisciplinary Studies, Rensselaer Polytechnic Institute, Troy, New York, USA

³Department of Biological Sciences, Rensselaer Polytechnic Institute, Troy, New York, USA

⁴Department of Chemical and Biological Engineering, Rensselaer Polytechnic Institute, Troy, New York, USA

⁵Department of Biological Engineering, Rensselaer Polytechnic Institute, Troy, New York, USA

⁶Department of Chemistry and Chemical Biology, Rensselaer Polytechnic Institute, Troy, New York, USA

⁷Shandong Institute for Food and Drug Control, Jinan, Shandong Province, China

Correspondence

Lianli Chi, National Glycoengineering Research Center, Shandong University, 72 Binhai Road, Qingdao, Shandong Province, 266237, China.

Email: lianlichi@sdu.edu.cn

Fuming Zhang, Center for Biotechnology and Interdisciplinary Studies, Rensselaer Polytechnic Institute, 110 8th Street, Troy, NY. 12180. USA.

Email: zhangf2@rpi.edu

Feng Shi, Shandong Institute for Food and Drug Control, 2749 Xinluo Avenue, Jinan, Shandong Province, 250101, China.

Email: 13953175123@139.com

Abstract

Background: Heparin-induced thrombocytopenia (HIT) is a serious complication caused by heparin drugs. The ultralarge complexes formed by platelet factor 4 (PF4) with heparin or low molecular weight heparins (LMWHs) are important participants in inducing the immune response and HIT.

Objectives: We aim at characterizing the interaction between PF4 and long-chain heparin oligosaccharides and providing robust analytical methods for the analysis of PF4-heparin complexes.

Methods: In this work, the characteristics of PF4-enoxaparin complexes after incubation in different molar ratios and concentrations were analyzed by multiple analytical methods, especially liquid chromatography-mass spectrometry and liquid chromatography-tandem mass spectrometry with multiple reaction monitoring were developed to qualitatively and quantitatively monitor heparin oligosaccharides and PF4 in HITinducing complexes.

Results: The results showed that the largest proportion of ultralarge complexes formed by PF4 and enoxaparin was at a specific molar ratio, ie, a PF4/enoxaparin ratio of 2:1, while the ultralarge complexes contained PF4 tetramer and enoxaparin at a molar ratio of approximately 2:1.

Conclusion: A binding model of PF4 and enoxaparin in ultralarge complexes is proposed with one heparin oligosaccharide chain (~ dp18) bound to 2 PF4 tetramers in different morphologies to form ultralarge complexes, while PF4 tetramer is surrounded by multiple heparin chains in smaller complexes. Our study provides new insights into the structural mechanism of PF4-LMWH interaction, which help to further understand the mechanism of LMWH immunogenicity and develop safer heparin products.

Manuscript handled by: Alan Mast

Final decision: Alan Mast, 18 August 2023

Deling Shi and Huimin Zhao contributed equally to this study as co-first authors.

© 2023 International Society on Thrombosis and Haemostasis. Published by Elsevier Inc. All rights reserved.

3608 J Thromb Haemost. 2023;21:3608-3618 jthjournal.org



Funding information

This work is supported by grants from the National Key R&D Program of China (2021YFF0600700), and GlycoMIP, a National Science Foundation Materials Innovation Platform funded through Cooperative Agreement DMR-1933525.

KEYWORDS

low molecular weight heparin, mass spectrometry, molecular docking simulation, platelet factor 4, thrombocytopenia

1 | INTRODUCTION

As an immune drug reaction, heparin-induced thrombocytopenia (HIT) occurs frequently when heparin and heparin-derived drugs are used clinically to prevent and treat pathologic coagulation [1]. HIT occurs in about 0.5% to 1% of medical and/or surgical patients receiving unfractionated heparin (mean molecular weight [MW] ~15 kDa) [2,3], leading to irreversible aggregation and depletion of blood platelets. HIT can be complicated by deep venous thrombosis or pulmonary embolism and can threaten a patient's life [4]. Likewise, HIT also occurs with the use of low molecular weight heparins (LMWHs, MW 3 kDa \sim 6 kDa), which are the products of controlled heparin degradation, by chemical or enzymatic means. LMWHs have more defined chemical and biological properties and lead to HIT in about 0.1% to 0.5% cases, less frequently than unfractionated heparin [4,5]. According to current understanding, HIT is caused by antibodies that recognize complexes formed by platelet factor 4 (PF4, also known as CXCL4) and heparin or LMWHs [6]. PF4, a basic protein synthesized and released by activated platelet α -particles, generally exists in the form of a tetramer, and the relative molecular weight of each PF4 monomer is 7.8 kDa [7]. PF4 combines with negatively charged heparin or LMWHs mainly through non-specific electrostatic binding to form PF4-heparin complexes that trigger the immune response to produce antibodies (eg, IgG). These antibodies tightly bind to the PF4heparin immune complexes, to form IgG-heparin-PF4 complexes, which can promote platelet activation and aggregation by binding with FCγRIIa receptor on platelets, resulting in increased platelet consumption and ultimately thrombocytopenia, and risk of venous and arterial thrombosis [8]. However, the mechanisms underlying the formation of PF4-heparin complexes have not been clearly identified.

PF4-heparin interaction is clinically significant, as the properties of the PF4-heparin complexes are closely related to the immune response and the occurrence of HIT. The shorter sugar chains in LMWHs or fondaparinux sodium have lower possibility to form the complexes with PF4 and produce less anti-PF4-heparin antibodies than those in heparin [9]. Ultralarge complexes (MW > 670 kDa), formed by PF4 tetramer and heparin/LMWHs, are central to the pathogenesis of HIT, and are formed in a narrow molar concentration range as demonstrated using size exclusion chromatography (SEC) [10,11]. Many techniques are used to report physicochemical characteristics of the PF4-heparin complexes, eg, binding affinity [12], average physical size, and surface charge [13,14]. Based on rupture forces and bond dynamics, a binding model for PF4-heparin complexes was proposed in which short

Essentials

- The U.S. Food and Drug Administration and the European Medicines Agency emphasize immunogenicity-related considerations for low molecular weight heparins.
- Liquid chromatography-tandem mass spectrometry with multiple reaction monitoring was developed to monitor low molecular weight heparins and platelet factor 4 in ultralarge complexes.
- PF4 and enoxaparin formed ultralarge complexes in a molar ratio approximately 2:1.
- Proposed binding model has heparin oligosaccharide (dp18) binding 2 PF4 tetramers.

heparins (≤8 saccharide units) bind to one PF4 tetramer, while long heparins bind to 2 PF4 tetramers [15]. The application of native mass spectrometry (MS) provides a more nuanced picture of the interaction of PF4 with short heparin chains (≤10 saccharide units), ie, each tetramer accommodates up to 6 pentasaccharides and longer polyanions can also induce PF4 dimer assembly when bound to the protein in relatively low numbers [16]. The crystal structures of fondaparinux sodium and PF4 tetramer support the hypothesis that heparin binds to more than one PF4 tetramer to form ultralarge complexes [17]. Even so, extrapolating the results obtained for short-chain oligosaccharides to longer chains remains challenging. Adequate detail about PF4-heparin interaction and robust analytical methods are still currently lacking due to the large molecular weight and complex structure of the PF4-heparin complexes.

Herein, we aim at characterizing the complexes formed by PF4 and enoxaparin sodium, the most commonly used LMWH in clinic and provide new insights into the binding ratio and mode of PF4 and long heparin oligosaccharides in the complexes. The particle size of the complexes formed by PF4 and enoxaparin or heparin at different concentrations are analyzed to obtain the molar ratio of reactants forming complexes. We address here the proportion of these complexes, especially the ultralarge complexes, and compare these using SEC. More importantly, liquid chromatography-mass spectrometry (LC-MS) and LC-MS/MS with multiple reaction monitoring (MRM) are developed to qualitatively and quantitatively monitor heparin oligosaccharides and PF4 in HIT-inducing complexes. Based on the binding molar ratio between PF4 and enoxaparin, a binding model of PF4 tetramer and heparin



oligosaccharide (dp18) is proposed in which one heparin chain binds to 2 PF4 tetramers in different morphologies to form ultralarge complexes, while multiple heparin chains bind one PF4 tetramer in smaller complexes. Our findings contribute to advancing the understanding of the interaction between PF4 and heparin products, and improving the immunogenicity evaluation and drug safety of heparin products.

2 | MATERIALS AND METHODS

2.1 | Materials

Enoxaparin sodium was purchased from Sanofi Winthrop Industrie and unfractionated heparin was obtained from the U.S. Pharmacopeia. Human PF4 was purchased from Abcam. Heparinase I, II, and III were purchased from Asnail Biotechnology Co, Ltd. 2-Aminoacridone (AMAC) was purchased from Sigma-Aldrich. Trypsin was obtained from Promega. All other chemicals and reagents were of high performance liquid chromatography (HPLC) grade.

2.2 Dynamic light scattering and zeta potential

The size and charge of PF4-heparin/enoxaparin complexes were measured using the Zetasizer Nano ZS90 equipped with a fixed 90 scattering angle and a helium-neon (He-Ne) laser (0.4 mW, 633 nm). In this experiment, the concentration of PF4 was 30 μ g/mL, and based on clinical dosage, enoxaparin sodium or heparin sodium was gradually added to the system, 0 international unit (IU)/mL, 0.22 IU/mL, 0.44 IU/mL, 0.87 IU/mL, 1.73 IU/mL, 3.46 IU/mL and 6.92 IU/mL, respectively. The contents and molar concentrations of heparin and enoxaparin can be calculated according to the drug instructions, heparin (217 IU/mg, MW = 16 kDa) and enoxaparin (100 IU/mg, MW = 4.5 kDa). Heparin or enoxaparin and PF4 were dissolved in HPLC grade water and incubated at 37 °C for 1 hour in different molar ratios and concentrations. Then the measurements were taken at 37 °C, and the size and Zeta potential measurements were reported as the average measurements of 3 fresh samples with 3 readings recorded per sample.

2.3 | Analysis of PF4-enoxaparin complexes using SEC

PF4 (0.1 mg/mL) and various amounts of enoxaparin (0-6.92 IU/mL) were dissolved in sodium phosphate buffer (pH 7.4; 10 mM). The mixture was then incubated at 37 °C for 60 minutes before injected into the Thermo U3000 HPLC system. The complexes were separated in an isocratic elution using the same phosphate buffer (pH 7.4; 10 mM) at 0.5 mL/min, 37 °C using a TSK Gel G5000PWXL (10 μm , 7.8 mm \times 300 mm) column. UV 210 nm and 232 nm wavelengths were selected to detect the complexes and other components. All experiments were repeated 3 times.

2.4 | Basic building block analysis of enoxaparin using hydrophilic interaction liquid chromatography-MS

Exhaustive enzymatic digestion was performed based on our previous method [18]. The disaccharides were determined using a hydrophilic interaction liquid chromatography-MS method carried out on a Thermo Scientific Ultimate 3000 UPLC and an LTQ Orbitrap XL FT mass spectrometer. The parameters were same as our previous work [19] with changes of step gradient: 0 to 20 minutes, 95% B; 20 to 122 minutes, 95% to 77% B; 122 to 127 minutes, 77% to 50% B; 127 to 150 minutes, 50% B. MS parameters were as follows: spray voltage, -4.2 kV; capillary voltage, -40 V; tube lens voltage, -50 V; capillary temperature, 275 °C; sheath flow rate, 30 arb; acquisition resolution, 60,000; and mass range, 240 to 800. The data were processed by using Thermo Xcalibur 3.0 software.

2.5 | MS/MS analysis of AMAC-labeled enoxaparin disaccharides

The enoxaparin disaccharides were labeled with AMAC [20]. MS and MS/MS analysis was performed on a SCIEX Triple Quad 6500+ mass spectrometer in negative ion mode. The MS/MS parameters were as follows: parent ion: Δ IS-AMAC, m/z (Q1): 384.5, z = -2, collision energy = -15 V, DP = 60 V; Δ IVA-AMAC, m/z (Q1): 572.2, z = -1, collision energy = -25 V, DP = 60 V; mass range, 100 to 800.

2.6 | LC-MS/MS MRM analysis of AMAC-labeled enoxaparin disaccharides

ExionLC UPLC system connected to a SCIEX Triple Quad 6500+ mass spectrometer was used to perform the LC-MS/MS MRM analysis. A Thermo BDS HYPERSIL C18 column (3 μ m, 150 mm \times 2.1 mm) was used. Mobile phase A was composed of 50 mM ammonium acetate in water, and methanol was used for mobile phase B. The gradient elution was 5% B for 2 minutes, 5% B to 55% B for 12 minutes, and 100% B for 8 minutes. The flow rate was set at 200 μ L/min, and the column temperature was 45 °C. The MRM transitions were optimized using the AMAC-labeled disaccharides. The final optimized conditions and collision energies for the all of the MRM transitions are as follows: MRM transitions: Δ IS-AMAC, m/z (Q1): 384.5, z = -2, m/z (Q3): 344.5, z = -2, collision energy: -15 V; Δ IVA-AMAC, m/z (Q1): 572.2, z = -1, m/z (Q3): 396.2, z = -1, collision energy: -25 V. The data were processed by SCIEX Analyst software.

2.7 LC-MS and LC-MS/MS analysis of PF4 peptides

Sequence analysis of PF4 was carried out based on our previous method [21]. Briefly, samples were mixed with denaturing buffer, then incubated with D,L-dithiothreitol and alkylated with iodoacetamide. Samples were digested with trypsin at an enzyme-to-protein ratio of 1/50 (w/w) at 37 °C for 12 hours. Nano-LC-MS/MS analysis was performed on a Thermo Easy-nanoLC and an Orbitrap Fusion Lumos

mass spectrometer equipped with a nanospray ion source. An Acclaim PepMap 100 trap column (2 cm \times 75 μ m, nano Viper 2Pk) and an Acclaim PepMap rapid separation liquid chromatography analytical column (25 cm \times 75 μ m, nano Viper, C18, 2 μ m) were used. Mobile phase A was 0.1% formic acid in 2% acetonitrile, and mobile phase B was 0.1% formic acid in 98% acetonitrile. The gradient elution was 2% to 7% B for 4 minutes, 7% to 22% B for 40 minutes, 22% to 35% B for 10 minutes, and 35% to 90% B for 5 minutes. The flow rate was set at 300 nL/min. The MS/MS parameters were set as follows: positive ion mode; capillary voltage, 2.1 kV; ion transfer tube temperature, 275 °C; ion spray voltage, 2,300 V; Orbitrap resolution, 120,000; scan range, 100 to 2000; quadrupole isolation window, 2; and collision energy, 30%; fragmentation, higher-energy collisional dissociation. The data were processed by Proteome Discoverer 3.0 software.

2.8 MS/MS and LC-MS/MS MRM analysis of PF4

Quantification analysis of PF4 was developed based on our previous method [21]. After reduction and alkylation, samples were digested with trypsin. The MS/MS and LC-MS/MS MRM analysis of PF4 was performed on a SCIEX Triple Quad 6500+ mass spectrometer in positive ion mode. The column was Thermo BDS HYPERSIL C18 (3.0 µm, 150 mm \times 2.1 mm). Mobile phase A was 0.1% formic acid in water, and mobile phase B was 0.1% formic acid in acetonitrile. The gradient elution was mobile phase 2% B for 5 minutes, 2% to 20% B for 3 minutes, 20% to 35% B for 12 minutes, 35% B for 3 minutes, and 98% B for 13 minutes. The flow rate was set at 0.15 mL/min. The MS/MS parameters were as follows: parent ion: TSQVRPR, m/z (Q1): 472.8, z = +2, collision energy = 35 V, DP = 60 V; HITSLEVIK, m/z (Q1): 520.3, z = +2, collision energy = 35 V, DP = 60 V; mass range, 100 to 1000. MRM transitions: TTSQVRPR, m/z (Q1): 472.8, z = +2, m/z (Q3): 742.4, z = +1, collision energy: 35 V; HITSLEVIK, m/z (Q1): 520.3, z = +2, m/z (Q3): 251.2, z = +1, collision energy: 35 V.

2.9 | Molecular modeling

The PF4 dimer structure (PDB: 4R9W) published by Cai et al. [17] was used to generate molecular models of a single tetramer and double tetramer structure. The protein-protein docking function in MOE2022 [22] was used to dock 2 dimers when generating the tetramer and then to dock 2 tetramers when generating the higher oligomeric structure. To complete the docking simulation, rigid body refinement was used along with 10000 pre-placement steps, 1000 placement steps and then 20 refined structures were retained. The lowest energy structures were then used to perform the docking experiment involving dp18 [23]. The general docking function in MOE2022 was used along with the induced fit refinement method to complete the docking of dp18 to the PF4 dimer and higher oligomeric species.

3 | RESULTS AND DISCUSSION

3.1 | Heterogeneity and molecular weight distribution of PF4-enoxaparin complexes formed at different PF4-enoxaparin ratio

Heparin, a mixture of negatively charged, linear polysaccharides extracted from porcine small intestinal mucosa, consists of repeating disaccharide units formed by $\alpha\text{-D-N-}acetylglucosamine}$ and $\alpha\text{-L-idur-}onic$ acid or $\beta\text{-D-}glucuronic}$ acid sugar residues that are modified with various sulfate groups [24]. Degradation of unfractionated heparin results in less polydisperse and smaller LMWHs, including enoxaparin sodium (mean MW $\sim\!4.5$ kDa), dalteparin sodium (mean MW $\sim\!6.0$ kDa) and nadroparin calcium (mean MW $\sim\!4.3$ kDa). Enoxaparin sodium is the most frequently prescribed LMWH worldwide, and is obtained by alkaline hydrolysis of benzyl esters of unfractionated heparin [25]. The size distribution of the complexes formed by PF4 and enoxaparin at different molar ratios was evaluated.

The Zetasizer Nano instrument, a user-friendly system for characterization of nanoparticles and macromolecules in solution, was used to analyze the size distribution profile of PF4-heparin/enoxaparin complexes. Size measurement was achieved by dynamic light scattering based on Brownian motion. Studies have shown that the patterns of PF4-heparin complexes remained the same when they were incubated at 37 °C for <2 hours [11]. In our study, PF4 and enoxaparin or heparin were incubated at 37 °C for 1 hour before analysis. The particle size measurement results are shown in Figure 1, Supplementary Tables S1 and S2. Confirming the literature data [13], we observed a bell-shaped relationship between heparin or enoxaparin concentration and complex size, and that enoxaparin was less likely to form larger complexes at the same concentration (Figure 1A). We also found that PF4 and enoxaparin formed large particle size, producing large complex molecule when mixed at the molar ratio of 2:1 (Figure 1B). The surface charge of the complexes, referred to as the Zeta potential, is another important indicator to evaluate the binding activity between LMWHs and PF4. When the molar ratio of PF4: enoxaparin is 2:1, the strongly negative Zeta potential value $(-34.5 \pm 1.7 \text{ mV})$ kept the particles stable in solution (Supplementary Table S3).

Then, the heterogeneity and molecular weight distribution of the complexes formed at different PF4/enoxaparin ratio (4:1, 2:1, and 1:1) were further analyzed using SEC (Figure 1C, Supplementary Tables S4 and S5). As shown in Figure 1C, enoxaparin and PF4 formed a complicated peak (retention time [RT] = 18-25 minutes) when PF4/enoxaparin ratio was 4:1. When adding more enoxaparin, a high molecular weight peak (RT = \sim 11.5 minutes) was observed at PF4/enoxaparin ratio 2:1 that accounted for 47 ± 2% of the total area. But this peak disappeared and another peak (RT = \sim 17.5 minutes) appeared when PF4/enoxaparin ratio was 1:1 and accounted for 27 ± 2% of the total area. Based on these results and other researchers' work [10,11], we speculated that the 2 newly emerged peaks were

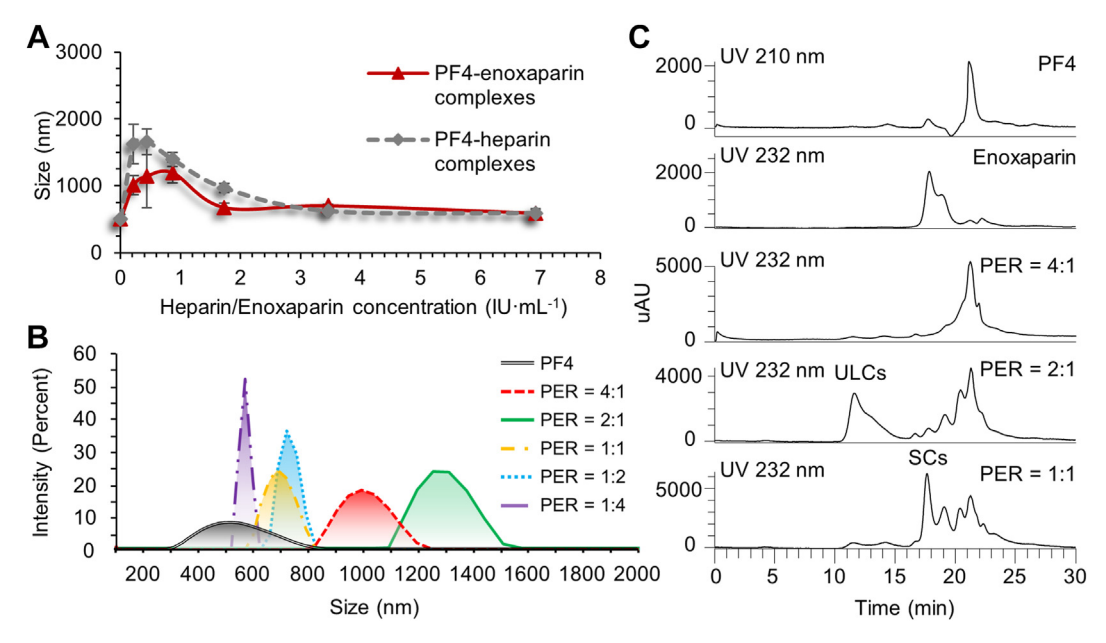


FIGURE 1 Size and size distribution of solutions containing PF4 and different concentrations of heparin/enoxaparin. (A) Particle size of complexes formed by PF4 and heparin/enoxaparin at different concentrations. (B) Particle size and size distribution of complexes formed by PF4 and enoxaparin at different PF4/enoxaparin ratio. (C) Size exclusion chromatography chromatograms of PF4 and enoxaparin mixture with different PF4/enoxaparin ratios. PF4, platelet factor 4; PER, PF4-enoxaparin molar ratio; ULCs, ultralarge complexes; SCs, smaller complexes.

ultralarge complexes (RT = \sim 11.5 minutes) and the smaller complexes (RT = \sim 17.5 minutes), while the peak (RT = 18-25 minutes) was a mixture of PF4/enoxaparin with no large molecular weight complexes formed. Here, the RT of enoxaparin (MW 4.5 kDa) is shorter than that of PF4 (the monomer is 7.8 kDa, but it may be in the form of tetramer). This may be because enoxaparin tends to exist in the form of long chain in solution, while PF4 protein tends to exist in the form of sphere. Another thing to be explained is that UV detection was performed using different wavelengths, 210 nm and 232 nm. PF4 absorbs at both wavelengths so these are not specific to either compound. Consequently, more specific analytical methods are required to further analyze the composition of each peak.

3.2 | Qualitative analysis of ultralarge and smaller complexes using high-resolution MS

High-resolution MS can provide definitive compositional information for each peak in the SEC chromatograms. We enriched the ultralarge complexes produced by 2:1 and smaller complexes produced by 1:1 mixture of PF4 and enoxaparin. Then the fractionated materials were evenly divided into 2 parts, and the components of enoxaparin and PF4 were analyzed, respectively. The samples were desalted and enzymatically hydrolyzed with 3K ultrafiltration membrane. Finally, the products under the membrane were collected after centrifugation, and qualitative analysis was performed using MS (Figure 2A).

Heparin is comprised of repeating disaccharide units of hexuronic acid residue (HexA) $1\rightarrow4$ linked to glucosamine residue (GlcN). The variability includes epimerization of HexA (either iduronic acid [doA] or glucuronic acid [GlcA]) and possible substitution at the 2-O-position

of HexA, 6-O-, 3-O-positions of GlcN, and/or the nitrogen of GlcN (NS or NAc). Enoxaparin is prepared by the chemical depolymerization of heparin, and the structure is shown in Figure 2B. After exhaustive enzymatic digestion, enoxaparin is broken down to its basic building blocks, and the backbone disaccharides include Δ IS (Δ UA2S-GlcNS6S), ΔIIS (ΔUA-GICNS6S), ΔIIIS (ΔUA2S-GICNS), ΔIVS (ΔUA-GICNS), ΔIA (ΔUA2S-GIcNAc6S), ΔΙΙΑ (ΔUA-GIcNAc6S), ΔΙΙΙΑ (ΔUA2S-GIcNAc), and ΔIVA (ΔUA-GlcNAc) [18] (structures shown in Supplementary Figure S1). In our study, main peaks of SEC chromatograms at different PF4/enoxaparin ratios were separated and exhaustively digested by heparinase I, II, and III before basic building blocks analysis using hydrophilic interaction liquid chromatography-MS (Figure 2C). Disaccharides analyzed by LTQ Orbitrap XL FT mass spectrometer with theoretical mass of disaccharide, observed m/z, charge state of detected molecules and the accuracy (ppm) were shown in Supplementary Table S6. Typical disaccharides were all identified in peak (RT = \sim 11.5 minutes) at PF4/enoxaparin ratio 2:1 and peak (RT = \sim 17.5 minutes) at PF4/enoxaparin ratio 1:1, which confirmed the presence of enoxaparin. Prior to MS analysis, PF4 was digested with trypsin to produce peptides. Trypsin specifically cleaves peptide bonds at the C-terminal side of lysine (K) and arginine (R) residues. PF4, sequence shown in Figure 2D, was digested into potential marker peptides, such as TTSQVRPR, HITSLEVIK, and EAEEDGDLQCLCVK (Figure 2E). The assigned peptide data including the confidence value (Xcorr) confirmed by Proteome Discoverer was shown in Supplementary Figure S2 and Table S7. C18-MS was used to detect these marker peptides in each peak of SEC chromatograms, which again confirmed the presence of PF4 in the peak (RT = \sim 11.5 minutes) at PF4/enoxaparin ratio 2:1 and peak (RT = \sim 17.5 minutes) at PF4/enoxaparin ratio 1:1. Using MS, we confirmed the presence of

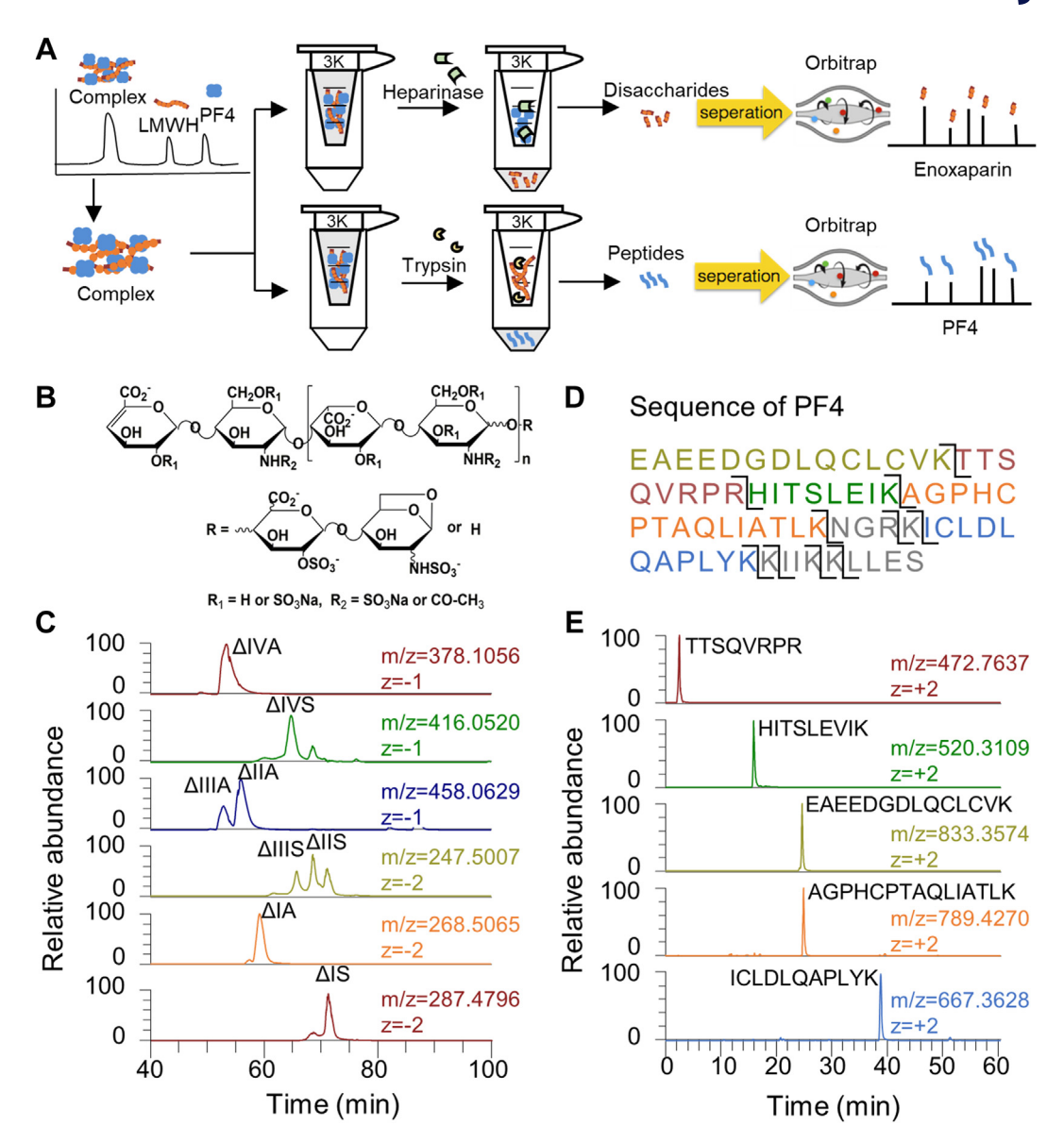


FIGURE 2 Qualitative analysis of complexes using high-resolution mass spectrometry. (A) Workflow of component identification for peaks obtained by size exclusion chromatography. (B) Structure of enoxaparin. (C) Disaccharides of enoxaparin analyzed by hydrophilic interaction liquid chromatography-MS in negative ion mode. (D) Sequence of PF4. (E) Peptides of PF4 detected by C18-MS in positive ion mode. PF4, platelet factor 4; MS, mass spectrometry.

ultralarge complexes (RT = \sim 11.5 minutes) and smaller complexes peak (RT = \sim 17.5 minutes).

3.3 | Quantitative analysis of the binding molar ratio of PF4 and enoxaparin in ultralarge and smaller complexes using LC-MS/MS MRM

The formation of ultralarge complexes is critical for the immunogenicity of heparin/LMWHs [10]. To elucidate the interaction between PF4 and enoxaparin and the formation of the complexes, ultralarge complexes formed at PF4/enoxaparin ratio 2:1 and smaller complexes formed at PF4/enoxaparin ratio 1:1 were separated and collected using SEC. LC-MS/MS MRM has been applied as the "gold standard"

method for quantification of both small molecules and large biomolecules [26]. In our work, complexes were collected, desalted, and digested using the same workflow as shown in Figure 2A, then LC-MS/ MS MRM was used to obtain the absolute content of PF4 and enoxaparin in the ultralarge and smaller complexes, respectively.

We chose 2 typical disaccharides of enoxaparin, Δ IS and Δ IVA, to measure the enoxaparin content. These disaccharides were labeled with AMAC to increase the intensity and shorten the analytical time [20], and the fragmentation patterns of MS/MS acquired by SCIEX Triple Quad 6500+ mass spectrometer were shown in Figure 3A, B. Product ions with high intensity and high specificity are used to establish MRM method. Based on the MS2 data, MRM transition 384.5>344.5 was applied to selectively monitor the AMAC-labeled Δ IS in the complexes in which 384.5 is doubly charged ion of

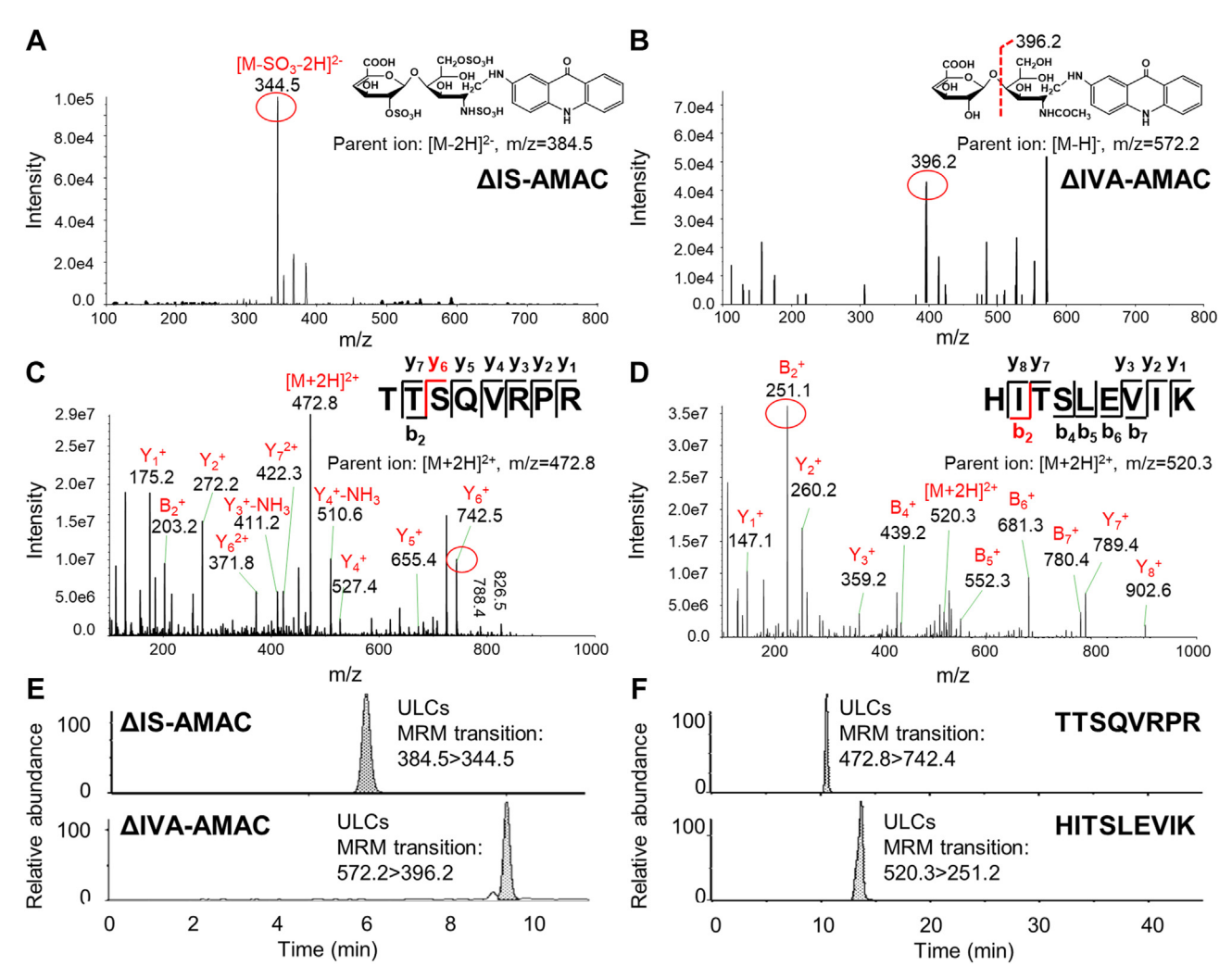


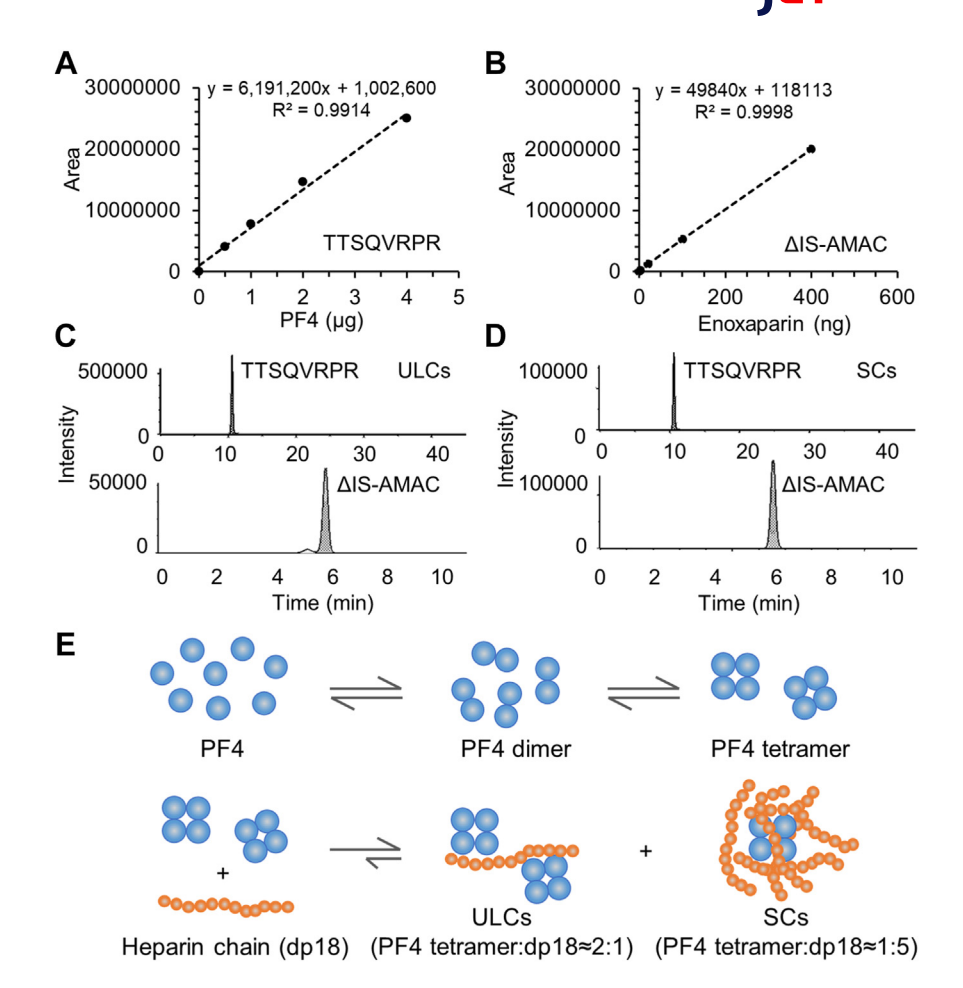
FIGURE 3 Monitoring enoxaparin and PF4 in HIT-inducing complexes using liquid chromatography-tandem mass spectrometry with multiple reaction monitoring obtained by SCIEX Triple Quad mass spectrometry. Tandem mass spectra of markers (A) Δ IS (Δ UA2S-GIcNS6S) -AMAC and (B) Δ IVA (Δ UA-GIcNAc) -AMAC analyzed in negative ion mode, (C) TTSQVRPR and (D) HITSLEVIK analyzed in positive ion mode. Multiple reaction monitoring transitions of (E) Δ IS-AMAC and Δ IVA-AMAC for enoxaparin detection and (F) TTSQVRPR and HITSLEVIK for PF4 detection. ULCs, ultralarge complexes. HIT, heparin-induced thrombocytopenia; PF4, platelet factor 4.

AMAC-labeled Δ IS in negative ion mode and 344.5 is an ion produced by neutral loss of sulfate group. For AMAC-labeled Δ IVA, the MRM transition is 572.0>396.2 in which 572.0 is doubly charged ion of AMAC-labeled ΔIVA in negative ion mode and 396.2 is an ion produced by loss of ΔUA residue. Likewise, the fragmentation patterns of MS/MS data acquired by SCIEX Triple Quad 6500+ mass spectrometer for 2 marker peptides of PF4, TTSQVRPR, and HITSLEVIK are shown in Figure 3C, D. The product ions were then chosen to develop LC-MS/MS MRM method to detect PF4 in the complexes. MRM transitions for TTSQVRPR is 472.8>742.4 in which 472.8 is doubly charged ion of TTSQVRPR in positive ion mode and 742.4 is single charge ion of SQVRPR. MRM transitions for HITSLEVIK is 520.3>251.2 in which 520.3 is doubly charged ion of HITSLEVIK in positive ion mode and 251.2 is single charge ion of HI minus OH group. Furthermore, 742.4 is chosen for its high specificity and better resistance to impurity interference, which is suitable for

quantification. While 251.2 is chosen for its high intensity and is suitable for qualitative analysis at low levels. Both the 2 transitions of enoxaparin and PF4 were used to analyze the ultralarge complexes to exclude false positives. LC-MS/MS MRM analysis for enoxaparin and PF4 were performed using different mobile phases and gradient conditions, and AMAC-labeled disaccharides were detected in negative ion mode and peptides in positive ion mode using SCIEX Triple Quad 6500+ mass spectrometer. Peaks were detected in all 4 transitions of the ultralarge complexes as shown in Figure 3E, F, again confirming that these are complexes of enoxaparin and PF4.

Quantification was carried out using components with higher content and better stability, and Δ IS was selected to quantify enoxaparin in the complexes, while TTSQVRPR was used to quantify PF4 in the complexes. The standard curves of LC-MS/MS MRM for both enoxaparin and PF4 showed good linearity (Figure 4A, B). The content of PF4 and enoxaparin in the ultralarge and smaller complexes was

FIGURE 4 Binding molar ratio and model of PF4 and enoxaparin in ultralarge and smaller complexes. Standard curve of (A) PF4 quantified by peptides TTSQVRPR and (B) enoxaparin quantified by AMAC-labeled ΔIS. Quantification of PF4 and enoxaparin in (C) ultralarge complexes and (D) smaller complexes by peptides TTSQVRPR and AMAC-labeled ΔIS. (E) The binding molar ratio of PF4 tetramer and enoxaparin in ultralarge complexes and smaller complexes. AMAC, 2-aminoacridone; PF4, platelet factor 4; SCs, smaller complexes; ULCs, ultralarge complexes.



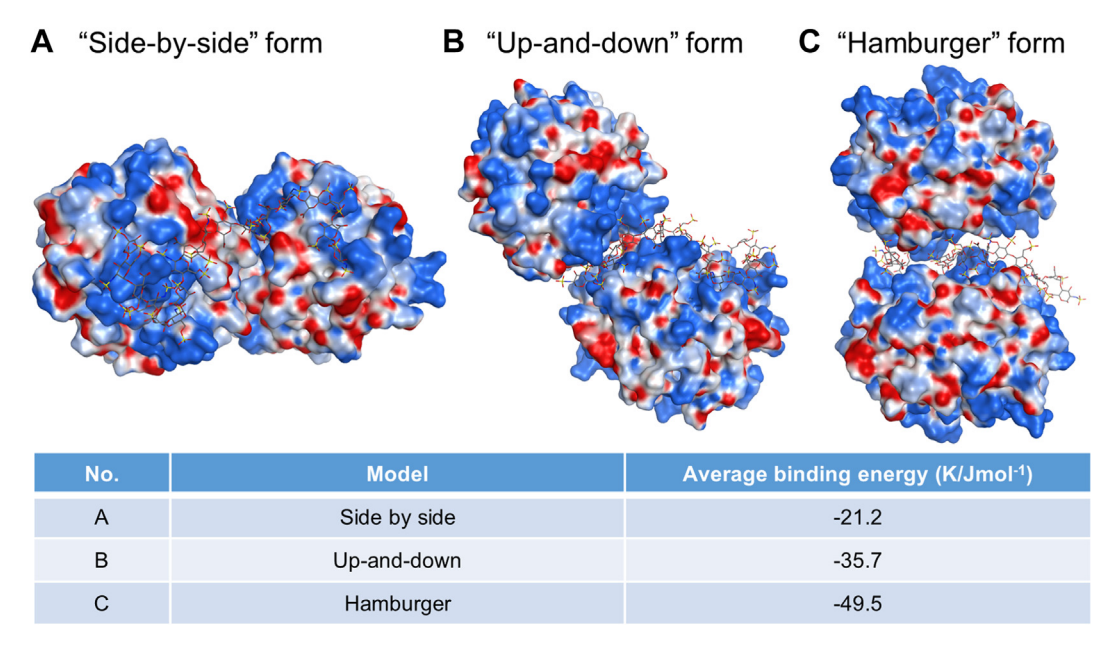


FIGURE 5 Three binding conformations and energy of PF4 tetramers in complex with the heparin oligosaccharide dp18. Conformations include (A) "side-by-side" form, (B) "up-and-down" form, and (C) "hamburger" form. In each conformation, the heparin oligosaccharide chain binds to 2 PF4 tetramers through electrostatic interactions via negatively charge oxygen atoms on heparin (red) interacting with positively charged pockets (blue clusters) on the tetramer surface. PF4, platelet factor 4.

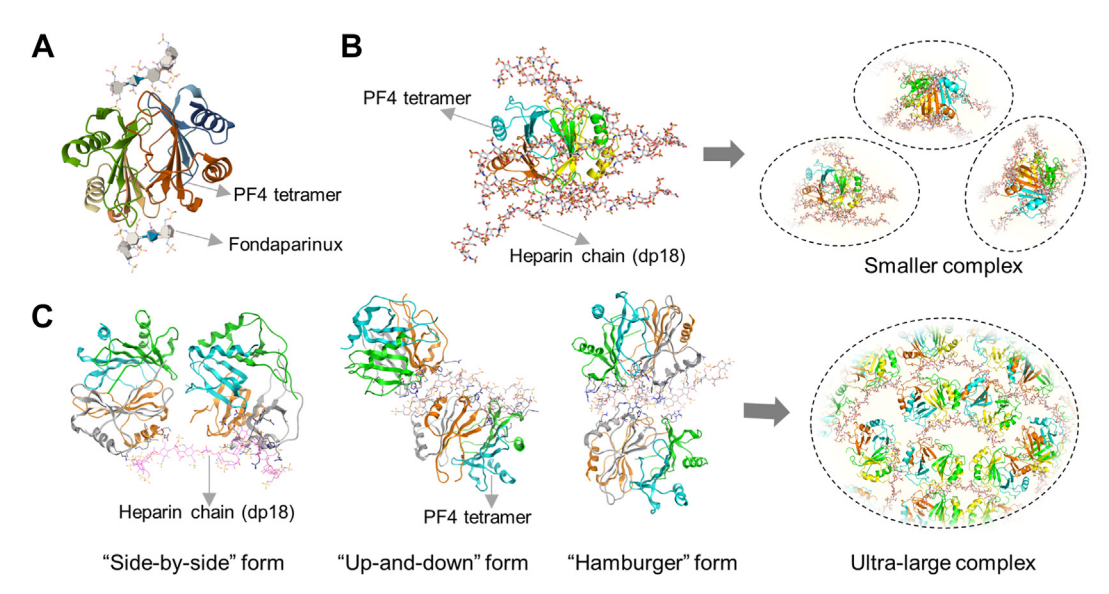


FIGURE 6 Proposed binding mode of heparin chains and PF4 tetramers. (A) PF4 complexed with short-chain heparin (PDB: 4R9W), (B) smaller complexes and (C) ultralarge complexes formed by PF4 tetramers and heparin chains. PF4, platelet factor 4.

calculated based on the LC-MS/MS MRM results (Figure 4C, D). PF4 can assume dimer and tetramer configurations (Figure 4E). The calculation formula is as follows.

$$PF4 \ tetramer : enoxaparin = \frac{m_{PF4}}{M_{PF4} \ tetramer} : \frac{m_{enoxaparin}}{M_{enoxaparin}}$$

 m_{PF4} is the content of PF4, M_{PF4} tetramer is the molecular weight of PF4 tetramer (M_{PF4} tetramer = 31200 Da), $m_{\text{enoxaparin}}$ is the content of enoxaparin, $M_{\text{enoxaparin}}$ is the average molecular weight of enoxaparin ($M_{\text{enoxaparin}}$ = 4500 Da).

The results demonstrated the binding molar ratio of PF4 tetramer and enoxaparin in ultralarge complexes was 2:1, while the binding molar ratio of PF4 tetramer and enoxaparin in smaller complexes was 1:5 (Supplementary Tables S8 and S9). There were slight differences in the quantitative results when selecting other peptides and disaccharides species. For example, the quantitative results of peptide EAEEDGDLQCLCVK were unstable due to disulfide bonds. For current LC-MS/MS MRM method, TTSQVRPR and AMAC-labeled ΔIS were more stable and ideal quantitative choices. The quantification results indicate that longer heparin chains, like enoxaparin (\sim dp18), are too long to just bind to one PF4 tetramer. Therefore, they are likely to bridge between 2 PF4 tetramers to find maximal binding partners to neutralize their negative charges (Figure 4E). For smaller complexes, PF4 tetramer was surrounded by multiple heparin chains, which inhibited the connection with other PF4 tetramers.

3.4 | Molecular modeling of binding model and sites of PF4 tetramers and long heparin chains

Despite our data accounting for the formation of the ultralarge complexes via a 2:1 molar ratio of PF4 tetramers and enoxaparin, we still lacked a molecular understanding of the conformations sampled in this state. To address this shortcoming, we developed a binding model of the PF4 tetramer and heparin oligosaccharide (dp18) in ultralarge complexes (Figure 5) in which one heparin chain is bound to 2 PF4 tetramers. The proposed binding model of PF4 and heparin oligosaccharide in ultralarge complexes is based on the binding molar ratio found in this study.

The PF4 dimer structure (PDB: 4R9W) was used to generate a single PF4 tetramer and double tetramer structure, and then used to analyze the interaction with dp18 (Supplementary Figure S3). From our molecular model, we were able to determine that the bound state of PF4 tetramers in complex forms with the heparin oligosaccharide dp18 can sample multiple conformations, namely "side-by-side" form (Figure 5A, Supplementary Figure S4), "up-and-down" form (Figure 5B, Supplementary Figure S5) and "hamburger" form (Figure 5C, Supplementary Figure Só). In general, the cluster of positively charged amino acids (R20, R22, H23, K31, H35, K46, R49, K61, K62, K65, K66) on the PF4 tetramer enables binding of the negatively charged dp18. Dp18 binding engages amino acids from each tetramer to stabilize the complex. Although different conformations of the complex can be formed, they will not be equally stable, as per the average binding energy shown Figure 5. The diverse combination modes enable the complexes to aggregate to form abundant ultralarge complexes. The existence and stability difference of the 3 binding forms make the ultralarge complexes diverse, which may explain the extensive molecular weight distribution of the ultralarge complex observed on the SEC chromatogram at PF4/enoxaparin ratio 2:1.

4 | CONCLUSION

HIT, a serious complication caused by heparin/LMWH products, can lead to thrombosis and embolism. The complexes formed from PF4

with heparin/LMWHs are important participants in inducing immune response and HIT. Properties of PF4-heparin/LMWHs complexes, including the particle size, surface charge, and amount of the complexes, can be impacted by the ratio and concentration of the 2 components. It is critical to study the formation of ultralarge and smaller complexes formed by PF4 and LMWHs to evaluate the immunogenicity of LMWHs and ensure the safety of medication.

In our work, after incubation at different ratios and concentrations, the characteristics of the complexes formed by PF4 and enoxaparin were studied using multiple analytical methods. The particle size, Zeta potential, and proportion of the complexes formed by PF4 and enoxaparin at different concentrations showed that the ultralarge complexes were easily formed at the PF4/enoxaparin ratio of 2:1. Moreover, qualitative and quantitative analysis of the ultralarge complexes using LC-MS and LC-MS/MS MRM revealed that PF4 tetramer and enoxaparin bind in a molar ratio of approximately 2:1, while the smaller complexes contained PF4 tetramer and enoxaparin at a molar ratio of approximately 1:5. A binding model is proposed based on the binding ratio discovered in our work and former crystal structure in which one heparin chain (dp18) is bound to 2 PF4 tetramers in ultralarge complexes, while PF4 tetramer is surrounded by multiple heparin chains in smaller complexes.

In this study, we propose a binding mode of heparin chains and PF4 tetramers (Figure 6), and visually demonstrate the process and differences in the formation of complexes between different heparin chains and PF4 tetramers. Short-chain lengths in fondaparinux and PF4 tetramers pose a challenge to form macromolecular complexes (Figure 6A), while long-chain heparin and PF4 tetramers can aggregate to form smaller (Fig. 6B) or ultralarge complexes (Figure 6C) at different molar ratios. Our study findings provide new insights into the interaction between PF4 and LMWHs, and afford a structural basis for further understanding the immunogenicity mechanism of LMWHs.

It can also be inferred that there will be differences in the binding ratio of heparin and other LMWHs to PF4 when forming complexes due to the differences in the chain length and structure. The formation of the complexes will reflect the immunogenicity of the heparin drugs and changing the structure of the heparin oligosaccharides or destroying the formation of the ultralarge complexes will help reduce the occurrence of HIT pathology. Future experiments aim at applying these methods to other heparin drugs and designing heparin analogs with reduced risk of HIT.

ACKNOWLEDGMENTS

This work is supported by grants from the National Key R&D Program of China (2021YFF0600700), and GlycoMIP, a National Science Foundation Materials Innovation Platform funded through Cooperative Agreement DMR-1933525.

AUTHOR CONTRIBUTIONS

L. Chi, F. Shi and F. Zhang designed the research; D. Shi, H. Zhao, C. Bu, K. Fraser and H. Wang performed the research; D. Shi and H. Zhao analyzed the data; D. Shi prepared the original draft; L. Chi, F. Zhang,

R. J. Linhardt and J. S. Dordick revised the manuscript; Funding was acquired by L. Chi, F. Shi, F. Zhang and R. J. Linhardt. All authors reviewed and approved the final version of the manuscript.

DECLARATION OF COMPETING INTERESTS

There are no competing interests to disclose.

REFERENCES

- [1] Cuker A, Arepally GM, Chong BH, Cines DB, Greinacher A, Gruel Y, Linkins LA, Rodner SB, Selleng S, Warkentin TE, Wex A, Mustafa RA, Morgan RL, Santesso N. American Society of Hematology 2018 guidelines for management of venous thromboembolism: heparininduced thrombocytopenia. *Blood Adv.* 2018;2:3360–92.
- [2] Dhakal B, Kreuziger LB, Rein L, Kleman A, Fraser R, Aster RH, Hari P, Padmanabhan A. Disease burden, complication rates, and healthcare costs of heparin-induced thrombocytopenia in the USA: a population-based study. *Lancet Haematol*. 2018;5:e220-e31.
- [3] Aguayo E, Sanaiha Y, Seo YJ, Mardock A, Bailey K, Dobaria V, Benharash P. Heparin-induced thrombocytopenia in cardiac surgery: incidence, costs, and duration of stay. Surgery. 2018;164: 1377–81.
- [4] Arepally GM, Padmanabhan A. Heparin-induced thrombocytopenia: a focus on thrombosis. Arterioscler Thromb Vasc Biol. 2021;41: 141–52.
- [5] Martel N, Lee J, Wells PS. Risk for heparin-induced thrombocytopenia with unfractionated and low-molecular-weight heparin thromboprophylaxis: a meta-analysis. *Blood*. 2005;106:2710–5.
- [6] Marchetti M, Zermatten MG, Bertaggia Calderara D, Aliotta A, Alberio L. Heparin-induced thrombocytopenia: a review of new concepts in pathogenesis, diagnosis, and management. J Clin Med. 2021;10:683.
- [7] Slungaard A. Platelet factor 4: a chemokine enigma. *Int J Biochem Cell Biol.* 2005;37:1162–7.
- [8] Ho PJ, Siordia JA. Dabigatran approaching the realm of heparininduced thrombocytopenia. *Blood Res.* 2016;51:77–87.
- [9] Warkentin TE, Cook RJ, Marder VJ, Sheppard JA, Moore JC, Eriksson BI, Greinacher A, Kelton JG. Anti-platelet factor 4/heparin antibodies in orthopedic surgery patients receiving antithrombotic prophylaxis with fondaparinux or enoxaparin. *Blood.* 2005;106: 3791-6.
- [10] Rauova L, Poncz M, McKenzie SE, Reilly MP, Arepally G, Weisel JW, Nagaswami C, Cines DB, Sachais BS. Ultralarge complexes of PF4 and heparin are central to the pathogenesis of heparin-induced thrombocytopenia. *Blood*. 2005;105:131–8.
- [11] Wu F, Dong K, Zhu M, Zhang Q, Xie B, Li D, Gan H, Linhardt RJ, Zhang Z. Development of a method to analyze the complexes of enoxaparin and platelet factor 4 with size-exclusion chromatography. J Pharm Biomed Anal. 2019;164:668–71.
- [12] Zhang F, Datta P, Dordick JS, Linhardt RJ. Evaluating heparin products for heparin-induced thrombocytopenia using surface plasmon resonance. J Pharm Sci. 2020;109:975–80.
- [13] Bertini S, Fareed J, Madaschi L, Risi G, Torri G, Naggi A. Characterization of PF4-heparin complexes by photon correlation spectroscopy and zeta potential. Clin Appl Thromb Hemost. 2017;23: 725–34.
- [14] Sommers CD, Ye H, Liu J, Linhardt RJ, Keire DA. Heparin and homogeneous model heparin oligosaccharides form distinct complexes with protamine: light scattering and zeta potential analysis. J Pharm Biomed Anal. 2017;140:113–21.
- [15] Nguyen TH, Greinacher A, Delcea M. Quantitative description of thermodynamic and kinetic properties of the platelet factor 4/heparin bonds. *Nanoscale*. 2015;7:10130–9.



- [16] Niu C, Yang Y, Huynh A, Nazy I, Kaltashov IA. Platelet factor 4 interactions with short heparin oligomers: implications for folding and assembly. *Biophys J.* 2020;119:1371–9.
- [17] Cai Z, Yarovoi SV, Zhu Z, Rauova L, Hayes V, Lebedeva T, Liu Q, Poncz M, Arepally G, Cines DB, Greene MI. Atomic description of the immune complex involved in heparin-induced thrombocytopenia. *Nat Commun.* 2015;6:8277.
- [18] Sun X, Sheng A, Liu X, Shi F, Jin L, Xie S, Zhang F, Linhardt RJ, Chi L. Comprehensive identification and quantitation of basic building blocks for low-molecular weight heparin. *Anal Chem.* 2016;88: 7738–44.
- [19] Zhang B, Shi D, Li M, Shi F, Chi L. A quantitative mass spectrometry method to differentiate bovine and ovine heparins from pharmaceutical porcine heparin. *Carbohydr Polym.* 2023;301: 120303.
- [20] Li G, Li L, Tian F, Zhang L, Xue C, Linhardt RJ. Glyco-saminoglycanomics of cultured cells using a rapid and sensitive LC-MS/MS approach. ACS Chem Biol. 2015;10:1303–10.
- [21] Li X, Shi F, Gong L, Hang B, Li D, Chi L. Species-specific identification of collagen components in Colla corii asini using a nano-liquid chromatography tandem mass spectrometry proteomics approach. *Int J Nanomedicine*. 2017;12:4443–54.

- [22] Molecular Operating Environment, 2022.02, Chemical Computing Group ULC, 1010 Sherbooke St. West, Suite #910, Montreal, QC, Canada, H3A 2R7, 2023.
- [23] Khan S, Gor J, Mulloy B, Perkins SJ. Semi-rigid solution structures of heparin by constrained X-ray scattering modelling: new insight into heparin-protein complexes. J Mol Biol. 2010;395:504–21.
- [24] Shriver Z, Capila I, Venkataraman G, Sasisekharan R. Heparin and heparan sulfate: analyzing structure and microheterogeneity. *Handb Exp Pharmacol*. 2012:159–76.
- [25] Mourier PAJ, Herman F, Sizun P, Viskov C. Analytical comparison of a US generic enoxaparin with the originator product: the focus on comparative assessment of antithrombin-binding components. J Pharm Biomed Anal. 2016;129:542–50.
- [26] Gianazza E, Tremoli E, Banfi C. The selected reaction monitoring/ multiple reaction monitoring-based mass spectrometry approach for the accurate quantitation of proteins: clinical applications in the cardiovascular diseases. Expert Rev Proteomics. 2014;11:771–88.

SUPPLEMENTARY MATERIAL

The online version contains supplementary material available at https://doi.org/10.1016/j.jtha.2023.08.020